Journal of Sound and Vibration (1997) **200**(1), 63–81

OUT-OF-PLANE VIBRATION OF A UNIFORM EULER–BERNOULLI BEAM ATTACHED TO THE INSIDE OF A ROTATING RIM

S. Naguleswaran

Department of Mechanical Engineering, University of Canterbury, Christchurch, New Zealand

(*Received* 3 *November* 1994, *and in final form* 26 *July* 1996)

This paper describes the out-of-plane vibration of a uniform Euler–Bernoulli beam one end of which is radially restrained (clamped or pinned) on the inside of a rotating rigid rim and the other end is radially unrestrained (clamped, pinned or free). Depending on the root offset parameter, the centrifugal axial force distribution may be wholly tensile or partly compressive and partly tensile or wholly compressive. The general solution of the mode shape differential equation is expressed as the superposition of four converging polynomial functions. Six combinations of clamped, pinned and free boundary conditions are considered, and the corresponding frequency equation is expressed in closed form, the roots of which give the natural frequencies. The first three out-of-plane dimensionless natural frequencies for typical combinations of the root offset parameter and rotational speed are presented in tabular form. Beyond a value of the root offset parameter, the frequencies increase and then decrease with increase in rotational speed. This aspect is discussed for the six combinations of the boundary conditions. It is possible for the rotational speed and a natural frequency to be equal (a "tuned" state) and for the beam to buckle at a critical rotational speed. These aspects are addressed and some representative results tabulated.

1. INTRODUCTION

This paper describes an investigation of the out-of-plane vibration of a uniform Euler–Bernoulli beam radially attached to the inside of a rigid rim which is rotating at a constant speed. The other end (radially unrestrained) will pass through or point towards the axis of rotation. Depending on the value of the root offset parameter (a measure of the root offset radius compared to the length of the beam) the centrifugal force distribution may be tensile over the whole length, compressive over part of the length and tensile over the remainder or compressive over the whole length. With increase in rotational speed, the natural frequency of vibration will either increase continously, or increase and then decrease continuously, or decrease continuously. In this study emphasis is placed on the latter. The "border" root offset parameter at which a natural frequency just decreases for an increase in rotational speed is derived numerically. If the root offset parameter is such that the frequency decreases, it is possible for a frequency to be zero at a critical rotational speed; i.e., buckling occurs. This problem is of practical and mathematical interest. Several investigators have derived the mode shape differential equation and devised various numerical methods to solve the dynamical behavior of a cantilever in a centrifugal field particularly the buckling aspect.

Mostaghel and Tadjbakhsh [1] used a method of successive approximation to estimate

0022–460X/97/060063 + 19 $25.00/0/sv960667

the rotational speed to cause a cantilever to buckle. Nachman [2] and Lakin [3] concentrated primarily on the mathematical aspects of the mode shape differential equation. Wang [4] used the Galerkin method with shape functions represented by a set of Legendre polynomials. Lakin *et al*. [5] had recourse to perturbation expansions in terms of several parameters appearing in the governing equation. Lakin and Nachman [6] studied the unstable vibrations and buckling of a flexible beam rotating rapidly (which causes one of the system parameters to be small) by a singular perturbation method. Fox and Burdess [7] used the Galerkin method to solve for natural frequencies, to obtain a "tuned" rotational speed which coincides with a natural frequency and to determine the radius of the rim for which a natural frequency is zero. White *et al*. [8] studied the in-plane and out-of-plane buckling of a cantilever using the integrating matrix method and presented a graph of the critical speed of rotation vs root offset parameter. Steele and Barry [9] used an asymptotic matrix integration method and presented graphs of the first two in-plane natural frequencies of a cantilever and the critical rotating speed. Peters and Hodges [10] developed asymptotic expansion formulae. Fox [11] reported the effect of the coupling between the motions in the two principal planes. Nachman [12] continued the study on the mathematical aspects discussed in references [2, 3] and developed a geometrically exact equation for a rotating cantilever. Kammer and Schlack [13] derived the critical rotational speed by the Liaponov's direct method. Subrahmanyam and Kaza [14] used the finite difference and the Ritz approach. Gürgöze [15] provided simple formulae from which one can calculate various approximate natural frequencies and the critical rotational speed. In references [1–15] there is broad qualitative agreement among the investigators but quantitative agreement is absent. In references [7, 11] it is stated that the mode shape differential equation "precludes an exact analytical solution". Eidel and Bauer [16] stated that "the partial differential equations permit no exact analytical solutions" and used the Ritz–Galerkin method with trinomials to obtain the approximate fundamental frequencies for combinations of free, clamped, hinged and guided boundaries. Wright *et al*. [17] studied a type of non-uniform beam under centrifugal tensile loading.

The mode shape differential equation was derived in references [1–15]. It is linear with variable coefficients, but no attempt was made in references [1–15] to solve it in the classical way; for example, by the method of Frobenius [18]. Naguleswaran [19] (a reference that lists a number of publications in which the centrifugal force distribution was tensile) used the method of Frobenius to solve the mode shape differential equation of a uniform Euler–Bernoulli beam attached radially to the outside of a rotating hub. This method is applied in the present paper. Some phenomena which occur in the problem discussed in the present paper are not mentioned in reference [19]. The six sets of boundary conditions are combinations of clamped (cl) or pinned (pn) at the rim end and clamped, pinned or free (fr) at the other end. The first three natural frequencies in dimensionless form for various combinations of the root offset parameter and speed of rotation are presented in tabular form to preserve the accuracy to four places after the decimal place. Graphs of the variation of the first two natural frequencies with rotational speed are presented for selected values of the root offset parameter. The "tuned" state (if any), i.e., when a rotational speed and a natural frequency coincide, are tabulated. Gyroscopic instruments for measuring the angular rates of turn based on this "tuned" state of a cantilever have been patented and are referred to in references [7, 11]. The critical rotational speed (if any) at which a natural frequency is zero (the Euler buckling condition) are tabulated for various root offset parameters. Some of the conclusions in past publications are shown to be erroneous. The "tuned" state and buckling do not occur in the problem discussed in reference [19].

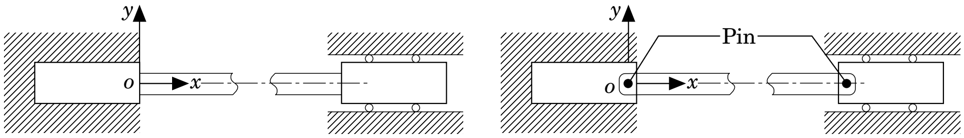

Figure 1. (a) Axially restrained (root) and (b) axially unrestrained boundaries.

2. THEORETICAL CONSIDERATIONS

Ideally clamped and pinned supports which are axially restrained or unrestrained are shown in Figure 1. Consider a uniform Euler–Bernoulli beam of flexural rigidity, EI, mass per unit length m and length l. In Figure 2 are shown the various positions at which the beam can be attached radially at a root offset radius R_0 from an axis rotating at a constant speed p. The origin is chosen at the point of attachment—the left end in the figure. The right end is radially unrestrained. The natural frequency of out-of-plane vibration of the beam shown in positions (a) and (b) of Figure 2 are tabulated in reference [19]. In the present paper positions (c)–(g) are considered. For position (a), the radial force $T(x)$ due to the centrifugal field at co-ordinate x is (a list of notation is given in Appendix B)

$$T(x) = 0{\cdot}5mp^2(l^2 + 2lR_0 - 2R_0x - x^2). \tag{1}$$

$T(x)$ is positive for tensile force and negative for compressive force. Equation (1) is applicable for the positions (c)–(g) of Figure 2, provided that R_0 is considered negative in these positions.

For out-of-plane natural vibration at frequency ω, if at co-ordinate x the amplitude of deflection, bending moment and transverse shearing force normal to the plane of rotation are $y(x)$, $M(x)$ and $Q(x)$, then

$$M(x) = EI\, \mathrm{d}^2y(x)/\mathrm{d}x^2, \qquad Q(x) = -\mathrm{d}M(x)/\mathrm{d}x + T(x)\, \mathrm{d}y(x)/\mathrm{d}x. \tag{2, 3}$$

The mode shape differential equation is

$$\mathrm{d}Q(x)/\mathrm{d}x + m\omega^2 y(x) = 0. \tag{4}$$

The derivation of equations (1–4) is given in Appendix A. The variables are expressed in dimensionless form as follows: the axial co-ordinate X, deflection $Y(X)$, the operator D,

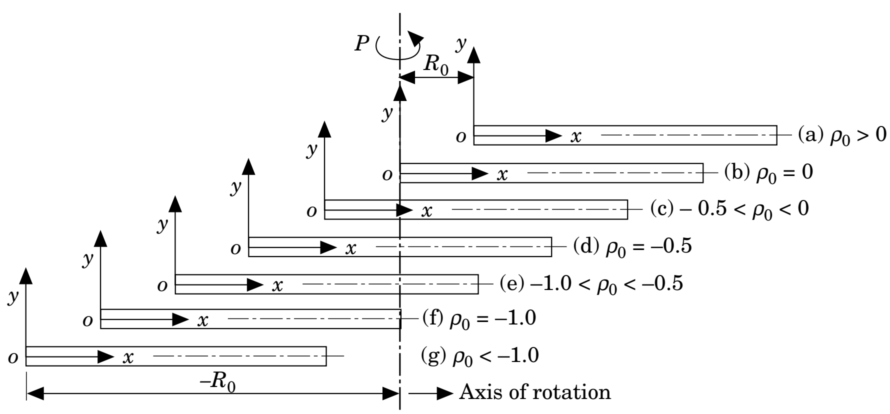

Figure 2. Positive and negative root offset parameters ρ_0.

the root offset parameter ρ_0, the rotational speed η, the tension $\beta(X)$, the natural frequency Ω, the bending moment $M(X)$ and shearing force $Q(X)$:

$$X = x/l, \qquad Y(X) = y(x)/l, \qquad D = \mathrm{d}/\mathrm{d}X, \qquad \rho_0 = R_0/l, \qquad \eta^2 = mp^2l^4/EI,$$

$$\beta(X) = T(x)l^2EI, \qquad \Omega^2 = m\omega^2l^4/EI, \qquad M(X) = M(x)l/EI, \qquad Q(X) = Q(x)l^2/EI. \quad (5)$$

The dimensionless radial force distribution due to the centrifugal field is

$$\beta(X) = 0{\cdot}5\eta^2(1 + 2\rho_0 - 2\rho_0X - X^2). \quad (6)$$

Equations (2) and (3) in dimensionless form are

$$M(X) = D^2Y(X), \qquad Q(X) = -D^3Y(X) + \beta(X)DY(X). \quad (7, 8)$$

The dimensionless mode shape differential equation is

$$D^4Y(X) - 0{\cdot}5\eta^2(1 + 2\rho_0)D^2Y(X) + \eta^2\rho_0D[XDY(X)]$$
$$+ 0{\cdot}5\eta^2D[X^2DY(X)] - \Omega^2Y(X) = 0. \quad (9)$$

Equation (9) with the boundary conditions is an eigenvalue problem. The six combinations of the boundary conditions considered in this paper are cl–cl, pn–pn, cl–pn, pn–cl, cl–fr and pn–fr (the first abbreviation denotes the boundary condition at the radially restrained end). The other combinations (fr–cl, fr–pn and fr–fr) are not of interest in engineering.

2.1. THE SOLUTION OF THE MODE SHAPE EQUATION

By following the method of Frobenius [18], the mode shape differential equation is found to have a solution of the form

$$F(X, c) = X^c \sum a_{n+1}(c)X^n, \qquad n = 0, 1, 2, \ldots, \infty, \quad (10)$$

in which the undetermined exponent c is the root of the indicial equation

$$c(c-1)(c-2)(c-3) = 0 \quad (11)$$

and the coefficients $a_{n+1}(c)$ satisfy the recurrence relationship

$$(c+n)(c+n-1)(c+n-2)(c+n-3)a_{n+1}(c) = 0{\cdot}5\eta^2(1+2\rho_0)$$
$$\times (c+n-2)(c+n-3)a_{n-1}(c)$$
$$+ \eta^2\rho_0(c+n-3)^2a_{n-2}(c) + [0{\cdot}5\eta^2(c+n-4)(c+n-3) - \Omega^2]a_{n-3}(c). \quad (12)$$

In equation (12), $a_1(c) = 1$ (arbitrary choice) and $a_m = 0$ for $m \leqslant 0$. The derivatives of $F(X, c)$ are

$$DF(X, c) = X^{c-1} \sum (c+n)a_{n+1}(c)X^n,$$

$$D^2F(X, c) = X^{c-2} \sum (c+n)(c+n-1)a_{n+1}(c)X^n \quad \text{and}$$

$$D^3F(X, c) = X^{c-3} \sum (c+n)(c+n-1)(c+n-2)a_{n+1}(c)X^n.$$

It is possible to compute the function $F(X, c)$ and the three derivatives progressively on a term-by-term basis. The four solution functions are

$$F(X, 0) = 1 + 0{\cdot}5\eta^2(1 + 2\rho_0)X^2/2 + \sum a_{n+5}(0)X^{n+4}, \quad (13)$$

$$F(X, 1) = X + 0{\cdot}5\eta^2(1 + 2\rho_0)X^3/6 - \eta^2\rho_0 X^4/24 + \sum a_{n+5}(1)X^{n+5}, \tag{14}$$

$$F(X, 2) = X^2 + 0{\cdot}5\eta^2(1 + 2\rho_0)X^4/12 - \eta^2\rho_0 X^5/30 + \sum a_{n+5}(2)X^{n+6}, \tag{15}$$

$$F(X, 3) = X^3 + 0{\cdot}5\eta^3(1 + 2\rho_0)X^5/20 - \eta^2\rho_0 X^6/40 + \sum a_{n+5}(3)X^{n+7}. \tag{16}$$

The four solution functions are clearly independent and hence the general solution of the mode shape differential equation is

$$Y(X) = C_1F(X, 0) + C_2F(X, 1) + C_3F(X, 2) + C_4(X, 3). \tag{17}$$

The constants of integration C_1, C_2, C_3 and C_4 are determined from the boundary conditions. For a clamped attachment, $Y(0) = 0 = DY(0)$. The mode shape function equation is

$$Y(X) = C_3F(X, 2) + C_4F(X, 3). \tag{18}$$

For a pinned attachment, $Y(0) = 0 = D^2Y(0)$. The mode shape function equation is

$$Y(X) = C_2F(X, 1) + C_4F(X, 3). \tag{19}$$

If at the axially unrestrained end $X = 1$ the beam is clamped, then $Y(1) = 0 = DY(1)$: if pinned, $Y(1) = 0 = D^2Y(1)$, and if free, $D^2Y(1) = 0 = D^3Y(1)$. The frequency equations for cl–cl, cl–pn, cl–fr, pn–cl, pn–pn and pn–fr beams are as follow:

cl–cl: $$F(1, 2)DF(1, 3) - DF(1, 2)F(1, 3) = 0, \tag{20}$$

cl–pn: $$F(1, 2)D^2F(1, 3) - D^2F(1, 2)F(1, 3) = 0, \tag{21}$$

cl–fr: $$D^2F(1, 2)D^3F(1, 3) - D^3F(1, 2)D^2F(1, 3) = 0, \tag{22}$$

pn–cl: $$F(1, 1)DF(1, 3) - DF(1, 1)F(1, 3) = 0, \tag{23}$$

pn–pn: $$F(1, 1)D^2F(1, 3) - D^2F(1, 1)F(1, 3) = 0, \tag{24}$$

pn–fr: $$D^2F(1, 1)D^3F(1, 3) - D^3F(1, 1)D^2F(1, 3) = 0. \tag{25}$$

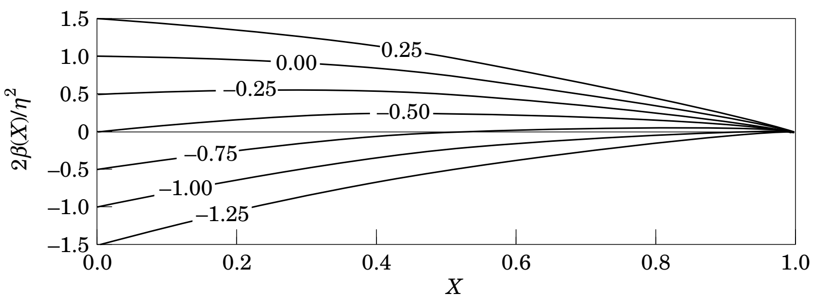

Figure 3. The axial centrifugal force distribution for various values of the root offset parameter ρ_0.

TABLE 1

The first three dimensionless natural frequencies for cl–cl *and for* pn–pn *uniform beams under centrifugal compression for various combinations of the rotational speed parameter η and the root offset parameter ρ_0*

		cl–cl beams				pn–pn beam			
	η	$\rho_0 = -0{\cdot}1$	$\rho_0 = -0{\cdot}5$	$\rho_0 = -1{\cdot}0$	$\rho_0 = -1{\cdot}5$	$\rho_0 = -0{\cdot}1$	$\rho_0 = -0{\cdot}5$	$\rho_0 = -1{\cdot}0$	$\rho_0 = -1{\cdot}5$
Ω_1	0	22·3733	22·3733	22·3733	22·3733	9·8696	9·8696	9·8696	9·8696
	1	22·4516	22·3967	22·3279	22·2589	9·9977	9·8986	9·7730	9·6454
	2	22·6844	22·4669	22·1911	21·9108	10·3711	9·9848	9·4748	9·9293
	3	23·0658	22·5831	21·9602	21·3138	10·9612	10·1268	8·9476	7·5458
	4	23·5869	22·7445	21·6309	20·4386	11·7306	10·3218	8·1320	4·8480
	5	24·2362	22·9497	21·1965	19·2354	12·6408	10·5664	6·8998	ccc
	6	25·0009	23·1971	20·6474	17·6180	13·6581	10·8568	4·8852	ccc
	7	25·8678	23·4850	19·9703	15·4254	14·7551	11·1888	ccc	ccc
	8	26·8237	23·8112	19·1463	12·2963	15·9109	11·5582	ccc	ccc
	9	27·8565	24·1736	18·1484	6·9259	17·1096	11·9607	ccc	ccc
	10	28·9547	24·5700	16·9360	ccc	18·3397	12·3924	ccc	ccc
	11	30·1084	24·9979	15·4453	ccc	19·5928	12·8496	ccc	ccc
	12	31·3088	25·4551	13·5646	ccc	20·8627	13·3290	ccc	ccc
	13	32·5483	25·9393	11·0650	ccc	22·1449	13·8274	ccc	ccc
	14	33·8204	26·4482	7·2729	ccc	23·4362	14·3424	ccc	ccc
	15	35·1196	26·9798	ccc	ccc	24·7340	14·8713	ccc	ccc
Ω_2	0	61·6728	61·6728	61·6728	61·6728	39·4784	39·4784	39·4784	39·4784
	1	61·7830	61·7085	61·6151	61·5216	39·6167	39·5169	39·3918	39·2662
	2	62·1122	61·8152	61·4414	61·0648	40·0282	39·6321	39·1303	38·6208
	3	62·6563	61·9926	61·1503	60·2932	40·7038	39·8232	38·6890	37·5148
	4	63·4085	62·2400	60·7392	59·1905	41·6292	40·0890	38·0593	35·8977

	5	63·3602	62·5562	60·2045	57·7318	42·7860	40·4278	37·2289	33·6885
	6	65·5006	62·9400	59·5411	55·8812	44·1535	40·8375	36·1802	30·7641
	7	66·8182	63·3898	58·7426	53·5873	45·7097	41·3156	34·8907	26·9469
	8	68·3001	63·9039	57·8010	50·7764	47·4326	41·8595	33·3311	22·0179
	9	69·9335	64·4804	56·7061	47·3399	49·3015	42·4662	31·4659	15·7586
	10	71·7054	65·1171	55·4422	43·1105	51·2967	43·1325	29·2546	6·8693
	11	73·6031	65·8118	54·0024	37·8116	53·4006	43·8553	26·6588	ccc
	12	75·6146	66·5622	52·3579	30·9280	55·5978	44·6314	23·6576	ccc
	13	77·7282	67·3659	50·4866	21·2017	57·8745	45·4574	20·2642	ccc
	14	79·9335	68·2205	48·3563	ccc	60·2190	46·3302	16·4992	ccc
	15	82·2206	69·1234	45·9252	ccc	62·6212	47·2466	12·2162	ccc
Ω_3	0	120·9034	120·9034	120·9034	120·9034	88·8264	88·8264	88·8264	88·8264
	1	121·0237	120·9419	120·8397	120·7373	88·9666	88·8667	88·7416	88·6164
	2	121·3838	121·0575	120·6482	120·2372	89·3855	88·9873	88·4866	87·9825
	3	121·9812	121·2499	120·3281	119·3976	90·0791	89·1879	88·0592	86·9133
	4	122·8121	121·5186	119·8777	118·2091	91·0402	89·4680	87·4559	85·3889
	5	123·8709	121·8631	119·2949	116·6579	92·2597	89·8266	86·6719	83·3798
	6	125·1511	122·2826	118·5767	114·7252	93·7262	90·2627	85·7004	80·8453
	7	126·6448	122·7763	117·7195	112·3864	95·4269	90·7751	84·5334	77·9647
	8	128·3434	123·3431	116·7188	109·6096	97·3479	91·3622	83·1605	73·9647
	9	130·2374	123·9818	115·5691	106·3537	99·4744	92·0226	81·5697	69·4560
	10	132·3169	124·6912	114·2641	102·5662	101·7914	92·7543	79·7466	64·0906
	11	134·5716	125·4699	112·7961	98·1798	104·2839	93·5554	77·6750	57·7296
	12	136·9910	126·3163	111·1564	93·1071	106·9372	94·4240	75·3361	50·2043
	13	139·5646	127·2289	109·3346	87·2351	109·7373	95·3578	69·7739	30·5662
	14	142·2822	128·2060	107·3185	80·4181	112·6708	96·3548	69·7739	30·5662
	15	145·1338	129·2457	105·0941	72·4733	115·7249	97·4125	66·5075	16·8810

ccc, Complex frequency; i.e., past buckling at this mode.

TABLE 2

As Table 1, but for cl–pn *and for* pn–cl *beams*

		cl–pn beams				pn–cl beam			
	η	$\rho_0 = -0{\cdot}1$	$\rho_0 = -0{\cdot}5$	$\rho_0 = -1{\cdot}0$	$\rho_0 = -1{\cdot}5$	$\rho_0 = -0{\cdot}1$	$\rho_0 = -0{\cdot}5$	$\rho_0 = -1{\cdot}0$	$\rho_0 = -1{\cdot}5$
Ω_1	0	15·4182	15·4182	15·4182	15·4182	15·4182	15·4182	15·4182	15·4182
	1	15·4991	15·4437	15·3741	15·3040	15·5368	15·4437	15·3262	15·2075
	2	15·7391	15·5199	15·2406	14·9551	15·8862	15·5199	15·0452	14·5498
	3	16·1299	15·6458	15·0145	14·3503	16·4481	15·6458	14·5585	13·3531
	4	16·6592	15·8199	14·6901	13·4476	17·1966	15·8199	13·8341	11·3908
	5	17·3122	16·0404	14·2584	12·1679	18·1026	16·0404	12·8145	7·9798
	6	18·0730	16·3049	13·7061	10·3493	19·1371	16·3049	11·3925	ccc
	7	18·9262	16·6106	13·0133	7·5670	20·2470	16·6106	9·3367	ccc
	8	19·8571	16·9547	12·1499	ccc	21·4912	16·9547	5·9178	ccc
	9	20·828	17·3342	11·0669	ccc	22·7704	17·3342	ccc	ccc
	10	21·9021	17·7462	9·6775	ccc	24·0971	17·7462	ccc	ccc
	11	22·9954	18·1877	7·7979	ccc	25·4601	18·1877	ccc	ccc
	12	24·1247	18·6558	4·8444	ccc	26·8505	18·6558	ccc	ccc
	13	25·2835	19·1479	ccc	ccc	28·2615	19·1479	ccc	ccc
	14	26·4663	19·6614	ccc	ccc	29·6881	19·6614	ccc	ccc
	15	27·6687	20·1939	ccc	ccc	31·1261	20·1939	ccc	ccc
Ω_2	0	49·9649	49·9649	49·9649	49·9649	49·9649	49·9649	49·9649	49·9649
	1	50·0751	50·0015	49·9093	49·8170	50·0993	50·0015	49·8789	49·7560
	2	50·4041	50·1113	49·7422	49·3698	50·5003	50·1113	49·6199	49·1227
	3	50·9469	50·2935	49·4619	48·6127	51·1608	50·2935	49·1839	48·0442
	4	51·6956	50·5474	49·0653	47·5262	52·0697	50·5474	48·5645	46·4837

	5	52·6400	50·8716	48·5484	46·0807	53·2126	50·8716	47·7521	44·3838
	6	53·7677	51·2645	47·9054	44·2317	54·5724	51·2645	46·7342	41·6614
	7	55·0655	51·7242	47·1289	41·9134	56·1308	51·7242	45·4940	38·2012
	8	56·5193	52·2486	46·2092	39·0261	57·8685	52·2486	44·0108	33·8548
	9	58·1150	52·8353	45·1343	35·4114	59·7667	52·8353	42·2595	28·4586
	10	59·8388	53·4820	43·8885	30·7966	61·8070	53·4820	40·2106	21·8268
	11	61·6774	54·1858	42·4519	24·6410	63·9724	54·1858	37·8325	13·1203
	12	63·6184	54·9442	40·7989	15·4602	66·2469	54·9442	35·0950	ccc
	13	65·6505	55·7543	38·8956	ccc	68·6165	55·7543	31·9778	ccc
	14	67·7631	56·6134	36·6971	ccc	71·0685	56·6134	28·4767	ccc
	15	69·9470	57·5188	34·1415	ccc	73·5915	57·5188	24·5916	ccc
Ω_3	0	104·2477	104·2477	104·2477	104·2477	104·2477	104·2477	104·2477	104·2477
	1	104·3683	104·2870	104·1852	104·0834	104·3859	104·2870	104·1631	104·0391
	2	104·7290	104·4046	103·9975	103·5883	104·7993	104·4046	103·9088	103·4102
	3	105·3271	104·6004	103·6834	102·7563	105·4844	104·6004	103·4830	102·3513
	4	106·1579	104·8739	103·2412	101·5766	106·4354	104·8739	102·8828	100·8461
	5	107·2154	105·2242	102·6685	100·0333	107·6444	105·2242	102·1039	98·8701
	6	108·4917	105·6506	101·9620	98·1045	109·1018	105·6506	101·1409	96·3094
	7	109·9782	106·1520	101·1175	95·7610	110·7967	106·1520	99·9869	93·3633
	8	111·6649	106·7272	100·1298	92·9645	112·7168	106·7272	98·6335	89·7327
	9	113·5415	107·3749	98·9928	89·6645	114·8491	107·3749	97·0705	85·4277
	10	115·5970	108·0934	97·6992	85·7947	117·1801	108·0934	95·2864	80·3609
	11	117·8202	108·8813	96·2400	81·2668	119·6962	108·8813	93·2675	74·4264
	12	120·2000	109·7367	94·6048	75·9618	122·3837	109·7367	90·9985	67·4992
	13	122·7251	110·6578	92·7813	67·7181	125·2292	110·6578	88·4623	59·4320
	14	125·3850	111·6426	90·7549	62·3153	128·2199	111·6426	85·6404	50·0351
	15	128·1691	112·6893	88·5082	53·4665	131·3434	112·6893	83·5132	39·0128

ccc, See Table 1.

TABLE 3

As Table 1, *but for* cl–fr *and for* pn–fr *beams*

		cl–fr beams				pn–fr beam			
	η	$\rho_0 = -0{\cdot}1$	$\rho_0 = -0{\cdot}5$	$\rho_0 = -1{\cdot}0$	$\rho_0 = -1{\cdot}5$	$\rho_0 = -0{\cdot}1$	$\rho_0 = -0{\cdot}5$	$\rho_0 = -1{\cdot}0$	$\rho_0 = -1{\cdot}5$
Ω_1	0	3·5160	3·5160	3·5160	3·5160	0·00†	0·00†	0·00†	0·00†
	1	3·6603	3·5735	3·4619	3·3465	0·9219	0·4996	ccc	ccc
	2	4·0610	3·7398	3·2938	2·7761	1·8438	0·9965	ccc	ccc
	3	4·6489	3·9993	2·9916	1·3694	2·7656	1·4885	ccc	ccc
	4	5·3584	4·3323	2·5047	ccc	3·6873	1·9738	ccc	ccc
	5	6·1435	4·7196	1·6743	ccc	4·6090	2·4510	ccc	ccc
	6	6·9751	5·1453	ccc	ccc	5·5305	2·9195	ccc	ccc
	7	7·8357	5·5972	ccc	ccc	6·4520	3·3793	ccc	ccc
	8	8·7147	6·0661	ccc	ccc	7·3734	3·8306	ccc	ccc
	9	9·6057	6·5456	ccc	ccc	8·2949	4·2740	ccc	ccc
	10	10·5048	7·0311	ccc	ccc	9·2163	4·7102	ccc	ccc
	11	11·4092	7·5195	ccc	ccc	10·1377	5·1399	ccc	ccc
	12	12·3175	8·0087	ccc	ccc	11·0590	5·5638	ccc	ccc
	13	13·2285	8·4973	ccc	ccc	11·9804	5·9826	ccc	ccc
	14	14·1416	8·9844	ccc	ccc	12·9018	6·3970	ccc	ccc
	15	15·0561	9·4695	ccc	ccc	13·8232	6·8073	ccc	ccc
Ω_2	0	22·0345	22·0345	22·0345	22·0345	15·4182	15·4182	15·4182	15·4182
	1	22·1615	22·0833	21·9852	21·8866	15·5947	15·4761	15·3263	15·1749
	2	22·5384	22·2293	21·8364	21·4360	16·1124	15·6484	15·0462	14·4163
	3	23·1530	22·4706	21·5854	20·6601	16·9391	15·9317	14·5641	13·0408
	4	23·9872	22·8044	21·2272	19·5152	18·0312	16·3205	13·8544	10·8012
	5	25·0191	23·2270	20·7545	17·9221	19·3423	16·8076	12·8751	7·0205

	6	26·2251	23·7338	20·1567	15·7313	20·8297	17·3850	11·5600	ccc
	7	27·5818	24·3197	19·4188	12·6098	22·4569	18·0440	9·8120	ccc
	8	29·0674	24·9792	18·5200	7·4057	24·1946	18·7757	7·5245	ccc
	9	30·6625	25·7064	17·4298	ccc	26·0194	19·5718	4·6703	ccc
	10	32·3499	26·4955	16·1028	ccc	27·9135	20·4241	ccc	ccc
	11	34·1152	27·3409	14·4671	ccc	29·8630	21·3255	ccc	ccc
	12	35·9460	28·2371	12·3974	ccc	31·8571	22·2694	ccc	ccc
	13	37·8320	29·1788	9·6396	ccc	33·8876	23·2499	ccc	ccc
	14	39·7648	30·1614	5·4332	ccc	35·9480	24·2621	ccc	ccc
	15	41·7372	31·1802	ccc	ccc	38·0332	25·3016	ccc	ccc
Ω_3	0	61·6972	61·6972	61·6972	61·6972	49·9649	49·9649	49·9649	49·9649
	1	61·8216	61·7408	61·6397	61·5384	50·1173	50·0115	49·8789	49·7459
	2	62·1931	61·8715	61·4667	61·0587	50·5716	50·1512	49·6199	49·0818
	3	62·8069	62·0886	61·1766	60·2483	51·3190	50·3831	49·1838	47·9496
	4	63·6553	62·3912	60·7671	59·0902	52·3458	50·7060	48·5644	46·3081
	5	64·7283	62·7781	60·2345	57·5577	53·6345	51·1180	47·7519	44·0917
	6	66·0137	63·2476	59·5740	55·6126	55·1649	51·6171	46·7336	41·2011
	7	67·4981	63·7978	58·7792	53·1996	56·9154	52·2005	45·4928	37·4877
	8	69·1673	64·4266	57·8424	50·2385	58·8642	52·8655	44·0085	32·7300
	9	71·0068	65·1315	56·7535	46·6089	60·9900	53·6089	42·2548	26·5948
	10	73·0022	65·9100	55·5004	42·1208	63·2726	54·4274	40·2015	18·4534
	11	75·1395	66·7593	54·0676	36·4484	65·6935	55·3174	37·8152	3·5012
	12	77·4054	67·6767	52·4363	28·9502	68·2359	56·2754	35·0629	ccc
	13	79·7875	68·6590	50·5823	17·9822	70·8846	57·2978	31·9199	ccc
	14	82·2741	69·7035	48·4754	ccc	73·6265	58·3810	28·3787	ccc
	15	84·8549	70·8071	46·0767	ccc	76·4498	59·5214	24·4446	ccc

ccc, See Table 1.

† Rigid body rotation.

3. CALCULATIONS

It was shown in reference [19] that if $\rho_0 \geqslant 0$ then $\beta(X) \geqslant 0$ and the natural frequency Ω increased with increase in the rotational speed η, and that a rotational speed does not exist for which $\Omega = \eta$. The present paper is a study of the influence of negative ρ_0 on the out-of-plane vibration. From equation (6), the variation of $2\beta(X)/\eta^2$ with X for various values of ρ_0 is shown in Figure 3. It is clear that $\beta(X) > 0$ for $0 > \rho_0 > -0{\cdot}5$ and hence, in this range of the root offset parameter, one can expect Ω to increase with η. A feature in the root offset parameter range $-1{\cdot}0 < \rho_0 < -0{\cdot}5$ is the centrifugal force distribution being compressive up to $X = -(1 + 2\rho_0)$ and tensile in the remainder of the beam. If the root offset parameter $\rho_0 = -2/3$, the total centrifugal force acting on the beam is zero. If $\rho_0 \leqslant -1{\cdot}0$, the centrifugal force distribution is compressive up to $X = 1$. A necessary (but not sufficient) condition for an out-of-plane natural frequency to decrease with increase in rotational speed is $\rho_0 < -0{\cdot}5$; i.e., part of the beam must be under centrifugal compression.

The roots of the frequency equations (20)–(25) were determined as follows. An initial trial and error search provided a narrow range for an approximate root. This was followed by an iterative procedure based on linear interpolation as described in reference [19]. The first three dimensionless (out-of-plane) natural frequencies Ω_1, Ω_2 and Ω_3 for combinations of $\rho_0 = -0{\cdot}1$, $-0{\cdot}5$, $-1{\cdot}0$ and $-1{\cdot}5$ ($\rho_0 = 0{\cdot}0$ is found in reference [19]) and η is the range 0 to 15 are tabulated in Table 1 for cl–cl and pn–pn beams, Table 2 for cl–pn and pn–cl beams, and Table 3 for cl–fr and pn–fr beams. The tabulation in Table 2 show that the natural frequency depends not only on the boundary conditions but also on which part of the boundary is radially restrained. For $\rho_0 = -0{\cdot}5$, the frequency columns for cl–pn and pn–cl beams are identical because, at this root offset, the centrifugal tension distribution is symmetrical. All of the frequency calculations in Tables 1–3 were in double precision on a VAX computer. Single precision calculation of the various functions in the frequency equations did not meet the accuracy required and, as a resullt, the iterative procedure failed. It was found that for some combinations of ρ_0 and η outside the parameters in the tables, double precision computing failed but quadruple precision computing succeeded, and for certain combinations even quadruple precision computing failed.

In Figures 4–6, the variation of Ω_1 and Ω_2 with η for the six combinations of boundary conditions are presented for selected (negative) values of ρ_0 with a view to determine the "border" root offset parameter at which Ω decreased or commenced to decrease with increase in η. White *et al*. [8] surmised that for a cl–fr beam this will happen if $\rho_0 = -0{\cdot}5 - \epsilon$, even if ϵ is very small but η is sufficiently large. The cl–fr beam frequency column in Table 3 for $\rho_0 = -0{\cdot}5$ and calculations with $\rho_0 = -0{\cdot}65$ (in Figure 6) show that Ω monotonically increased with η. Wang [4] investigated the same problem and suggested that the "border" $\rho_0 = -0{\cdot}778$. The cl–fr beam first mode frequency variation shown in Figure 6 shows that the Wang suggestion is in error. In reference [7] it was suggested that if $\rho_0 = -0{\cdot}64$, Ω increases with η and if $\rho_0 = -0{\cdot}66$, Ω decreases with η if $\eta > 14$. Kammer and Schlack [13] suggested the "border" $\rho_0 = -0{\cdot}642$. Presently, analytical technique is not available to predict this "border" root offset parameter. The "border" root offset parameters tabulated in Table 4 were obtained numerically—the criterion used is that in the range $15 < \eta < 20$, the variation in Ω is less than $0{\cdot}5\%$.

From Figures 4–6, it is possible to derive the conditions for a natural frequency to coincide with the rotational speed. Fox and Burdess [7] called this a "tuned" state and calculated (by the Galerkin procedure) the "tuned" rotational speeds of a cantilever. (A stroboscope will show a "frozen" no-node cantilever at the first "tuned" rotational

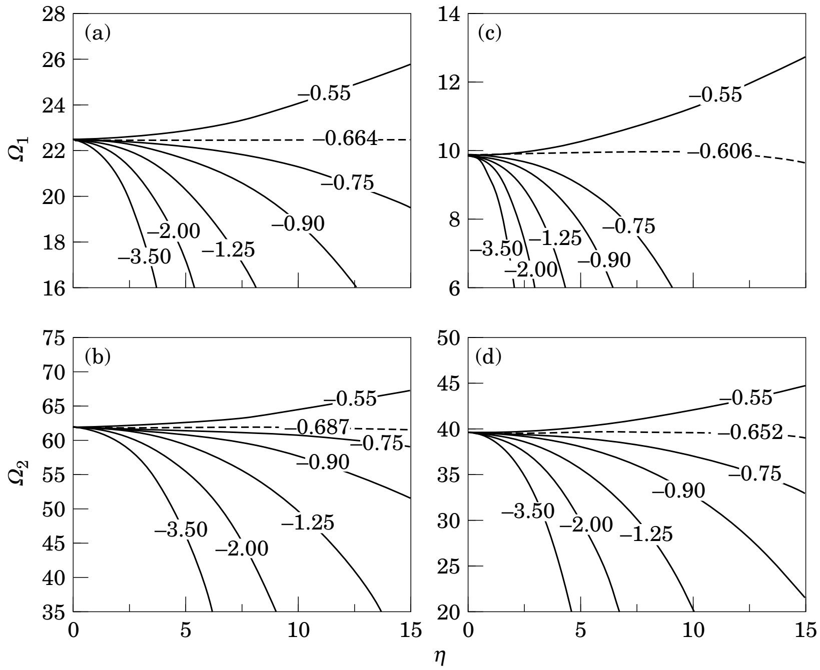

Figure 4. The variation of the first two dimensionless natural frequencies of cl–cl and of pn–pn beams with rotational speed η for various negative root offset parameters ρ_0. The broken line is the estimated "border" root offset parameter. (a) cl–cl mode 1; (b) cl–cl mode 2; (c) pn–pn mode 1; (d) pn–pn mode 2.

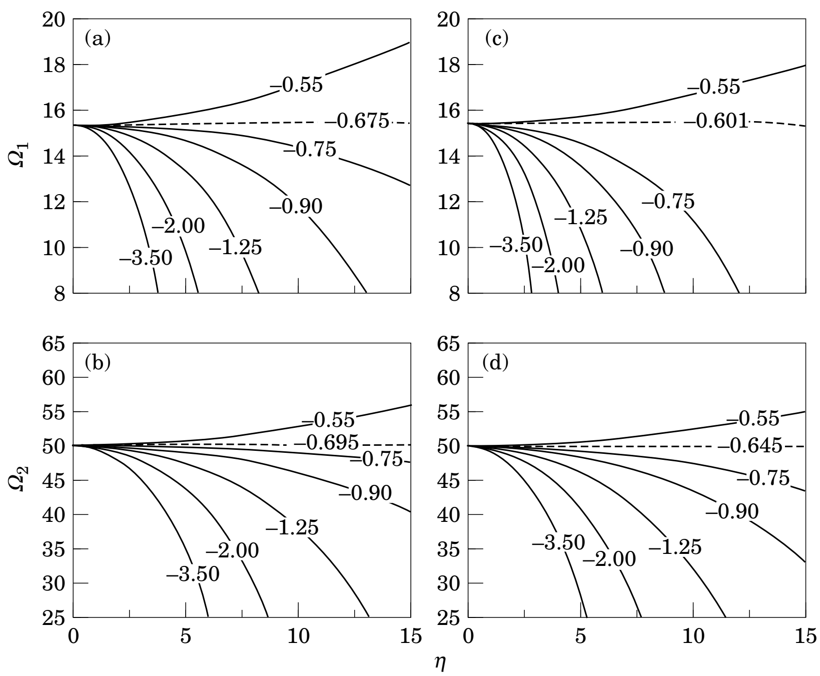

Figure 5. As Figure 4, but for cl–pn and of pn–cl beams, respectively.

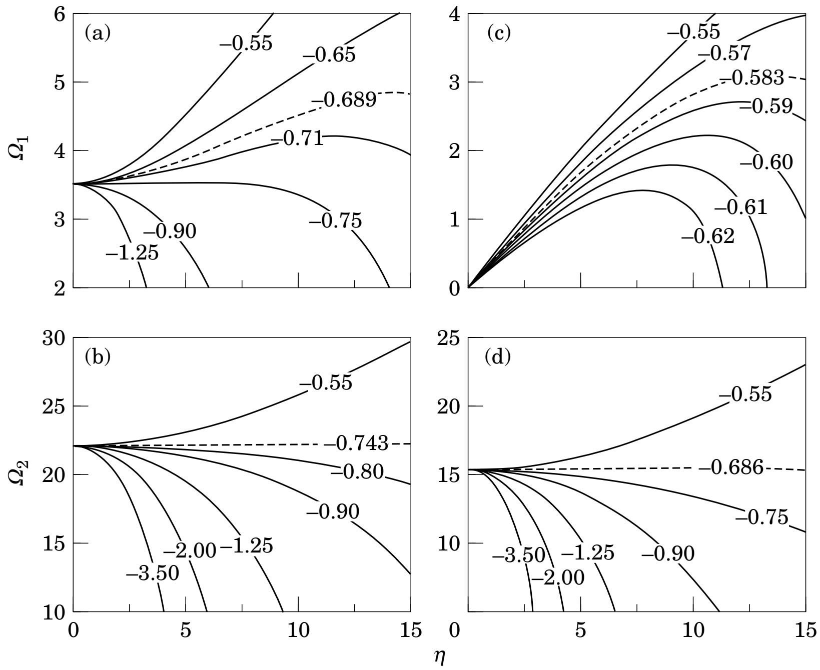

Figure 6. As Figure 4, but for cl–fr and of pn–fr beams, respectively.

speed η_{t1}, a "frozen" one-mode cantilever at the second "tuned" speed η_{t2} and so on.) Provided that the system is ideal, there is nothing special in this phenomena. However, an imperfection such as a slight tilt in the "circular" path of the attachment will cause a displacement excitation at the rim end which will result in a dangerous resonance response. A small radial eccentricity in the attachment may cause parametric instability, but this falls outside the scope of this paper. The differential equation to be solved for the "tuned" rotational speed η_t is

$$D^4Y(X) - \eta_t^2\{0{\cdot}5(1+2\rho_0)D^2Y(X) - \rho_0 D[XDY(X)] - 0{\cdot}5D[XC^2DY(X)] - Y(X)\} = 0. \tag{26}$$

This equation subject to the boundary conditions forms an eigenvalue problem. The eigenvalues (viz., η_t^2) if negative indicate that "tuned" rotational speeds do not exist. The "tuned" rotational speed equations are of the same form as equations (20)–(25) and the roots are calculated by the iterative procedure. In Table 5, the first two "tuned" rotational speeds for the six combinations of boundary conditions are tabulated. Results published

Table 4

The estimated "border" root offset parameter ρ_0 at which Ω just tends to decrease with increase in η

	The "border" root offset parameter					
	cl–cl	pn–pn	cl–pn	pn–cl	cl–fr	pn–fr
Mode 1	−0·664	−0·606	−0·675	−0·601	−0·689	−0·583
Mode 2	−0·687	−0·652	−0·695	−0·645	−0·743	−0·686

TABLE 5

The first two dimensionless "tuned" rotational speeds η_{t1} and η_{t2} for various root offset parameters ρ_0

	ρ_0	cl–cl	pn–pn	cl–pn	pn–cl	cl–fr	cl–fr†	pn–fr
η_{t1}	−0·60	nc	10·1430	18·6818	15·4280	4·0450	[7]	***
	−0·70	19·9604	8·1641	14·6553	11·5957	3·6845	—	***
	−0·80	16·2356	7·0124	12·4002	9·6548	3·4048	3·5	***
	−0·90	13·9979	6·2391	10·9276	8·4404	3·1798	3·2	***
	−1·00	12·4756	5·6747	9·8741	7·5908	2·9939	3·0	***
	−1·25	10·1275	4·7412	8·1687	6·2421	2·6417	2·7	***
	−1·50	8·7414	4·1547	7·1191	5·4244	2·3899	2·5	***
	−2·00	7·1113	3·4332	5·8484	4·4440	2·0466	2·1	***
	−2·50	6·1467	2·9913	5·0799	3·8550	1·8183	1·9	***
	−3·00	5·4912	2·6853	4·5516	3·4514	1·6265	1·7	***
	−3·50	5·0087	2·4573	4·1598	3·1527	1·5251	1·5	***
η_{t2}	−0·60	**	**	**	**	25·3553	—	23·1133
	−0·70	nc	nc	nc	nc	22·4471	—	14·5606
	−0·80	26·2756	20·1414	28·2742	23·7398	17·7401	19·5	10·8683
	−0·90	22·5734	16·6347	21·2628	19·2517	14·1632	15·5	9·0167
	−1·00	20·5770	14·4902	18·7760	16·7170	12·1171	12·3	7·8655
	−1·25	16·0406	11·4359	14·5170	13·1366	9·3777	9·5	6·2174
	−1·50	13·5181	9·7425	12·2347	11·1673	7·9283	8·1	5·3001
	−2·00	10·7517	7·8283	9·7392	8·9538	6·3329	6·6	4·2609
	−2·50	9·1933	6·7265	8·3293	7·6852	5·4294	5·6	3·6619
	−3·00	8·1\610	5·9883	7·3949	6·8375	4·8284	5·0	3·2604
	−3·50	7·4130	5·4497	6·7176	6·2198	4·3915	4·5	2·9674

† From reference [7]
, Expected to be large; nc, not calculated; *, does not exist.

TABLE 6

The first two dimensionless critical rotational speeds η_{c1} and η_{c2} for various root offset parameters ρ_0

	ρ_0	cl–cl	pn–pn	cl–pn	pn–cl	cl–fr	cl–fr†		pn–fr
η_{c1}	−0·60	**	**	**	**	**	[7]	[8]	15·4740
	−0·70	26·1675	nc	nc	16·2418	30·3746	17·0	20·0	us
	−0·80	22·0247	9·5931	19·3454	11·9450	11·1689	11·5	10·3	us
	−0·90	17·3370	7·8635	14·9521	9·8563	7·2842	7·3	7·6	us
	−1·00	14·6849	6·8175	12·5684	8·5747	5·6747	5·6	5·6	us
	−1·25	11·2122	5·3506	9·1563	6·7573	3·9900	4·0	4·0	us
	−1·50	9·4111	4·5469	7·9597	5·7527	3·2566	3·3	3·3	us
	−2·00	7·4581	3·6468	6·2883	4·6193	2·5159	2·6	2·6	us
	−2·50	6·3664	3·1282	5·3602	3·9678	2·1237	2·1	—	us
	−3·00	5·6461	2·7830	4·7499	3·5316	1·8715	1·9	—	us
	−3·50	5·1254	2·5316	4·3095	3·2135	1·6920	1·7	—	us
η_{c2}	−0·60	**	**	**	**	**	—	—	**
	−0·70	nc	nc	nc	nc	nc	—	—	nc
	−0·80	39·0749	nc	nc	nc	nc	—	—	nc
	−0·90	29·4798	19·6179	21·7319	21·5223	18·8993	18·0	—	12·7412
	−1·00	21·3070	16·3911	19·8684	18·3496	14·4902	14·7	—	9·8741
	−1·25	16·6548	12·3124	15·2223	13·8924	10·3118	10·5	—	7·0076
	−1·50	13·8791	10·2687	12·6517	11·6210	8·4707	8·4	—	5·7462
	−2·00	10·9303	8·0939	9·9417	9·1826	6·6049	6·7	—	4·4745
	−2·50	9·3040	6·8926	8·4545	9·8283	5·6009	5·6	—	3·7926
	−3·00	8·2381	6·1048	7·4820	6·9376	4·9494	5·0	—	3·3507
	−3·50	7·4706	5·5371	6·7826	6·2949	4·4828	4·5	—	1·9938

† From references [7, 8].
**, Expected to be large; nc, not calculated; us, unstable.

on "tuned" frequencies are for cl–fr beams and values from graph of η_t versus ρ_0 from reference [7] (Galerkin method) are included in Table 5 for comparison. Where $\eta_t > 20$, the values were not calculated and this is shown by *nc*, and the values shown by ** (if they exist) are expected to be very large.

For the combinations of ρ_0 and η for which Ω decreases with increase in η, a critical η_c exists for which a natural frequency is zero, and the beam will buckle at this mode. The differential equation to be solved is

$$D\{D^3Y(X) - \eta_c^2[0{\cdot}5(1 + 2\rho_0)DY(X) - \rho_0 XDY(X) - 0{\cdot}5X^2DY(X)]\} = 0. \qquad (27)$$

This equation, together with the boundary conditions, forms an eigenvalue problem and the buckling speed equations are of the same form as equations (20)–(25). The first two buckling speeds for the six combinations of the boundary are tabulated in Table 6. Included in Table 6 are results for cl–fr beams from graphs in references [7] and [8]. Where $\eta_c > 20$, calculations were not done and this is shown by *nc* and if buckling is unlikely or if η_c is expected to be very large, are shown by **.

4. CONCLUSIONS

The first three dimensionless natural frequencies for out-of-plane vibration of a uniform Euler–Bernoulli beam attached to the inside of a rotating rim have been tabulated for six combinations of clamped, pinned and free boundary conditions and for various values of the root offset parameter. For $\rho_0 \geqslant -0{\cdot}5$ the centrifugal axial force distribution is tensile and Ω increases with increase in η. For $-1{\cdot}0 < \rho_0 < -0{\cdot}5$ the axial force distribution is partly compressive. For $\rho_0 = -0{\cdot}5 - \epsilon$, where ϵ is small, Ω increased with moderate increase in η and one would expect the frequency to decrease if η is large but the precision with which the computer operated precluded verification. If ϵ is not small, Ω decreases monotonically. For $\rho_0 < -1{\cdot}0$, the centrifugal force distribution is compressive and Ω decreases monotonically. The above aspects are illustrated in Figures 4–6. For $\eta < 20$, the first two "border" root offset parameters obtained numerically are presented in Table 4.

A "tuned" state is possible when $\Omega = \eta$. Imperfections may lead to dangerous resonance and hence the "tuned" state must be avoided. Some values of "tuned" rotational speeds are presented in Table 5.

For certain combinations of ρ_0 and η, a frequency may be zero, resulting in buckling of the beam. Some values of the critical rotational speeds are presented in Table 6.

REFERENCES

1. N. Mostaghel and I. Tadjbakhsh 1973 *International Journal of Mechanical Sciences* **15**, 429–434. Buckling of rotating rods and plates.
2. A. Nachman 1954 *Journal of Applied Mechanics* **42**, 222–224. The buckling of rotating rods.
3. W. D. Lakin 1976 *Journal of Engineering Mathematics* **10**, 313–321. Vibrations of a rotating flexible rod clamped off the axis of rotation.
4. J. T. S. Wang 1976 *International Journal of Mechanical Sciences* **18**, 407–411. On the buckling of rotating rods.
5. W. D. Lakin, R. Mathon and A. Nachman 1978 *Journal of Engineering Mathematics* **12**, 193–206. Buckling of a rotating spoke.
6. W. D. Lakin and A. Nachman 1978 *Quarterly of Applied Mathematics* **35**, 479–493. Unstable vibrations and buckling of rotating flexible rods.
7. C. H. J. Fox and J. S. Burdess 1979 *Journal of Sound and Vibration* **65**, 151–158. The natural frequencies of a thin rotating cantilever with offset root.
8. W. F. White, R. G. Kvaternik and K. R. V. Kaza 1979 *International Journal of Mechanical Sciences* **21**, 739–745. Buckling of rotating beams.

9. C. R. Steele and K. E. Barry 1980 *Journal of Applied Mechanics* **47**, 884–890. Asymptotic integration methods applied to rotating bars.
10. D. A. Peters and D. H. Hodges 1980 *Journal of Applied Mechanics* **47**, 398–402. In-plane vibration and buckling of a rotating beam clamped off the axis of rotation.
11. C. H. J. Fox 1985 *Journal of Sound and Vibration* **98**, 325–336. The free vibration of compact rotating radial cantilevers.
12. A. Nachman 1986 *Journal of Sound and Vibration* **109**, 435–443. Buckling and vibration of a rotating beam.
13. D. C. Kammer and A. L. Schlack Jr. 1986 *Journal of Vibration, Acoustics, Stress, and Reliabilty in Design* **108**, 389–393. Critical spin rate of rotating beams by Liapunov's direct method.
14. K. B. Subrahmanyam and K. R. V. Kaza 1986 *Journal of Vibration, Acoustics, Stress, and Reliability in Design* **108**, 140–149. Vibration and buckling of rotating, pretwisted, preconed beams including Corriolis effects.
15. M. Gürgöze 1990 *Journal of Sound and Vibration* **143**, 356–363. On the dynamical behaviour of a rotating beam.
16. H. F. Bauer and W. Eidel 1988 *Journal of Sound and Vibration* **122**, 357–375. Vibration of a rotating beam, part II: orientation perpendicular to the axis of rotation.
17. A. D. Wright, C. E. Smith, R. W. Thresher and J. L. C. Wang 1982 *Journal of Applied Mechanics* **49**, 197–202. Vibration modes of centrifugally stiffened beams.
18. F. B. Hildebrand 1976 *Advanced Calculus for Applications*. Englewood Cliffs, NJ: Prentice-Hall; second edition.
19. S. Naguleswaran 1994 *Journal of Sound and Vibration* **175**, 613–624. Lateral vibration of a centrifugally tensioned uniform Euler–Bernoulli beam.
20. A. W. Leissa 1996 *Private communication*.

APPENDIX A: THE GOVERNING EQUATIONS

It is gratefully acknowledged that this Appendix is based on notes provided by Professor A. W. Leissa in a private communication [20]. An element of the beam is undeflected and in a typical deflected position is shown in Figure A1. Here s is the curvilinear co-ordinate

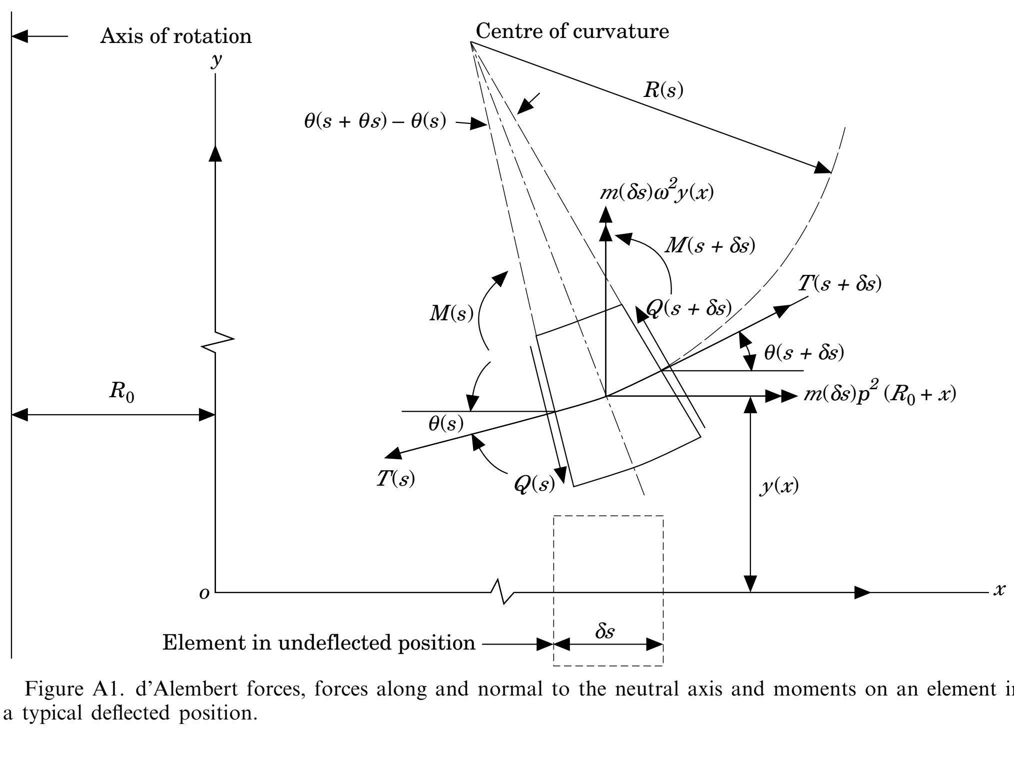

Figure A1. d'Alembert forces, forces along and normal to the neutral axis and moments on an element in a typical deflected position.

along the neutral axis. The free body diagram shows the force $T(s)$ along the neutral axis, the shearing force normal to the neutral axis and the d'Alembert forces. For small deflection the Euler–Bernoulli equation for bending is

$$M(s) = EI/R(s) \approx EI\, \mathrm{d}^2 y(x)/\mathrm{d}x^2, \tag{A1}$$

where $R(s)$ is the radius of curvature at s. Considering the equilibrium of the element one gets

$$\mathrm{d}[T(s)\cos\theta(s) - Q(s)\sin\theta(s)]/\mathrm{d}s + mp^2(R_0 + x) = 0 \tag{A2}$$

$$\mathrm{d}[T(s)\sin\theta(s) + Q(s)\cos\theta(s)]/\mathrm{d}s + m\omega^2 y(x) = 0, \tag{A3}$$

$$Q(s) + \mathrm{d}M(s)/\mathrm{d}s = 0. \tag{A4}$$

The tension $T(x)$ in the radial direction and the shearing force $Q(x)$ in the transverse direction are

$$T(x) = T(s)\cos\theta(s) - Q(s)\sin\theta(s), \qquad Q(x) = T(s)\sin\theta(s) + Q(s)\cos\theta(s),$$

$$Q(s) = -T(x)\sin\theta(s) + Q(s)\cos\theta(s) \approx -T(x)\,\mathrm{d}y(s)/\mathrm{d}s + Q(x). \tag{A5}$$

For small deflection, $M(s) \approx M(x)$, d/ds $\approx$ d/dx and equations (1–4) are obtained.

APPENDIX B: NOTATION

$a_{n+1}(c)$	coefficient of X^{c+n} in $Y(X, c)$
c	roots of indicial equation (11)
$C_{1,2,3,4}$	constants of integration in equation (17)
D, D^n	operators $\mathrm{d}/\mathrm{d}X$, $\mathrm{d}^n/\mathrm{d}X^n$
EI	flexural rigidity of beam
$F(X, c)$	trial solution function, equation (10)
$F(X, c)_{c=0,1,2,3}$	the four solution functions of, equation (9)
l	length of beam
m	mass per unit length of beam
$M(s)$	amplitude of moment at curvilinear co-ordinate s
$M(x)$	amplitude of bending moment, equation (2)
$M(X)$	dimensionless amplitude of bending moment, equation (5)
p	rotational speed about axis
$Q(s)$	amplitude of shearing force normal to neutral axis
$Q(x)$	amplitude of shearing force normal to plane of rotation, equation (3)
$Q(X)$	dimensionless amplitude of shearing force, equation (5)
R_0	radius of rim; i.e., root offset radius
$R(s)$	radius of curvature of the deflected element
s	curvilinear co-ordinate along neutral axis
$T(s)$	force along neutral axis at s
$T(x)$	radial force at co-ordinate x, equation (1)
x	axial co-ordinate
X	dimensionless axial co-ordinate, equation (5)
$y(x)$	amplitude of deflection

$Y(X)$	dimensionless amplitude of deflection, equation (5)
$\beta(X)$	dimensionless axial tension, equation (5)
ω	a natural frequency
Ω	dimensionless natural frequency, equation (5)
$\Omega_{1,2,3}$	first, second and third natural frequency
η	dimensionless rotational speed, equation (5)
η_c	buckling rotational speed (i.e.m $\Omega = 0$) in equation (27)
η_t	"tuned" rotational speed (i.e., $\eta_t = \Omega$) in equation (26)
ρ_0	root offset parameter, equation (5)
$\sum$	summation from 0 to ∞